European Journal of Medicinal Chemistry 85 (2014) 487–497

Contents lists available at ScienceDirect

European Journal of Medicinal Chemistry

journal homepage: http://www.elsevier.com/locate/ejmech

Original article

Design, synthesis and biological evaluation of novel 1-hydroxyl-3-aminoalkoxy xanthone derivatives as potent anticancer agents

Zheng-Min Yang [a], Jun Huang [a], Jiang-Ke Qin [a, *], Zhi-Kai Dai [b, *], Wen-Li Lan [a], Gui-Fa Su [a], Huang Tang [a], Feng Yang [a]

[a] Key Laboratory for the Chemistry and Molecular Engineering of Medicinal Resources, School of Chemistry and Pharmaceutical Sciences, Guangxi Normal University, Guilin 541004, PR China
[b] Department of Pharmacology, Guilin Medical University, Guilin 541004, PR China

ARTICLE INFO

Article history:
Received 22 November 2013
Received in revised form
21 July 2014
Accepted 21 July 2014
Available online 22 July 2014

Keywords:
Xanthone
Synthesis
Anticancer activity
Structure–activity relationships
Apoptosis
Intracellular calcium
Mitochondrial membrane potential

ABSTRACT

A series of novel 1-hydroxyl-3-aminoalkoxy xanthone derivatives were designed, synthesized and evaluated for *in vitro* anticancer activity against four selected human cancer cell lines (nasopharyngeal neoplasm CNE, liver cancer BEL-7402, gastric cancer MGC-803, lung adenocarcinoma A549). Most of the synthesized compounds exhibit effective cytotoxic activity against the four tested cancer cell lines with the IC_{50} values at micromolar concentration level. Some preliminary structure–activity relationships were also discussed. In this series of derivatives, compound **3g** shows excellent broad spectrum anticancer activity with IC_{50} values ranging from 3.57 to 20.07 μM. The *in vitro* anticancer activity effect and action mechanism of compound **3g** on human gastric carcinoma MGC-803 cell were further investigated. The results showed that compound **3g** exhibits dose- and time-dependent anticancer effects on MGC-803 cells through apoptosis, which might be associated with its decreasing intracellular calcium and the mitochondrial membrane potential.

1. Introduction

Xanthone, also named 9*H*-xanthene-9-one, is a fundamentally structural framework of active ingredients isolated from many medicinal plants and microorganism. It has a planar tricyclic skeleton, in which one pyran ring is fused with two phenyl rings on both sides (Fig. 1). Owing to this kind of simple and interesting structural scaffolds and variable substituents on the rings, xanthone derivatives show broad pharmacological activities such as antioxidant activity [1,2], anticancer activity [3,4], α-glucosidase inhibitory activity [5], antibacterial and antifungal activity [6]. Their interesting structural scaffold and pharmacological importance have attracted many scientists to isolate or synthesize these compounds as novel drug candidates [3].

In recent years, the development of xanthone derivatives as effective anticancer drug candidates has attracted considerable attention, lots of natural or synthetic xanthone compounds possessing excellent antiproliferative activities were obtained [4,7,8]. Younghwa Na and his co-workers reported a series of epoxypropoxy-substituted xanthone derivatives which show significant cytotoxic, topoisomerase inhibitory and DNA cross-linking activities [9–11]. Due to the planar pharmacophore structure of the xanthone, its anticancer activity was related with its interaction with DNA and can be dramatically altered by the ring substituents and their positions [3]. Though the biological mechanism of action has not been thoroughly investigated, some xanthone derivatives are currently undergoing clinical trials for cancer treatment. Among them, an impressive natural xanthone analogue is psorospermin (Fig. 1), the xanthone group can interact with DNA base pairs, while the epoxide group can alkylate N7-guanine of DNA in the presence of topoisomerase II [12,13]. Another synthetic xanthone known as antitumor drug candidates is 5,6-dimethylxanthone-4-acetic acid (DMXAA) (Fig. 1). This compound could interact with diverse biological targets via various actions and it had entered phase II clinical trials and shown promising activity against malignant tumors [14–16].

Modifying natural compounds with efficient synthetic methods and calibrating their pharmacologically active structure were regarded to be a key method to find new anticancer drug. In

* Corresponding authors.
E-mail addresses: jiangkeq@sina.com, jiangkeq@163.com (J.-K. Qin), dzhk110@126.com (Z.-K. Dai).

http://dx.doi.org/10.1016/j.ejmech.2014.07.076
0223-5234/

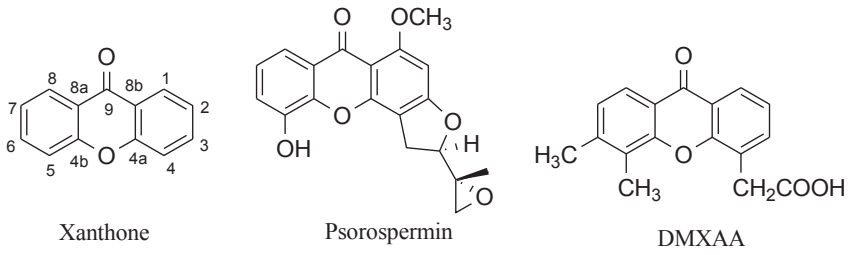

Fig. 1. Chemical structures of some reported xanthone derivatives.

previous works of our groups [17,18] and others [9], 1,3-dihydroxylxanthone could be used as an important lead compound for chemical modification to obtain potent anticancer candidates. The physicochemical and biological activities of a pharmacophore could usually be improved by the introduction of a nitrogen-containing side chain. Considering that aminoalkoxy groups are conveniently introduced onto 1,3-dihydroxyxanthone's pharmacophore via simple etherification and amination reactions, a series of novel 1,3-dihydroxyxanthone derivatives with their terminal amines linked by different carbon spacers were designed, synthesized and evaluated for their anticancer activity *in vitro*. The primary aim of this work was to gain some insight into the effect of terminal amines and linker length on the anticancer activities of these compounds, and further indicate an interesting structure–activity relationship for the search of potential anticancer drugs. In addition, cell and molecular biological experiments, such as cell growth curves, morphological examination and colonial measurement, etc., were carried out to further investigate the anticancer effects of the most potent compound **3g** on human gastric carcinoma MGC-803 cell and the preliminary mechanism was also discussed.

2. Results and discussion

2.1. Chemistry

The synthetic route of 1-hydroxyl-3-aminoalkoxy xanthone derivatives is shown in Scheme 1. 1,3-dihydroxylxanthone was obtained in a yield of 52% from the condensation reaction of salicylic acid with phloroglucinol in the presence of anhydrous zinc chloride and phosphorus oxychloride [17–19]. Later, the etherification of the hydroxyl group in the position 3 of 1,3-dihydroxyxanthone with 1,ω-dibromoalkane was carried out in K_2CO_3/acetone to offer the key intermediates **2a**–**2e**, which possessed various side chains with different length. Then, compounds **2a**–**2e** were treated with appropriate alkyl amines in ethanol under reflux to yield the target compounds **3a**–**3i**, which were finally quaternized with methyl iodide in chloroform to obtain the corresponding quaternary ammonium salts **4a**–**4i** with improved water solubility. The twenty-three new compound **2a**–**2e**, **3a**–**3i**, **4a**–**4i** were characterized by elemental analysis, IR, NMR and MS. The NMR assignments were provided explicitly in the section of spectral data.

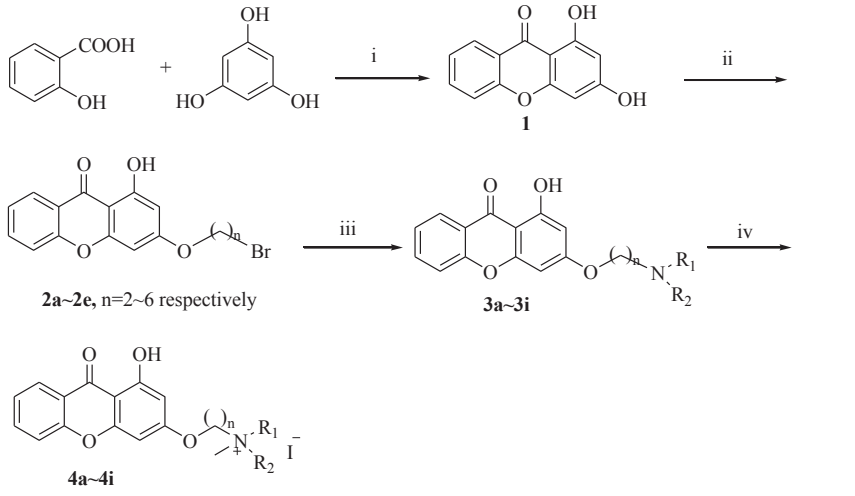

	a	b	c	d	e	f	g	h	i
n	2	3	4	5	6	4	4	4	4
$-N^{R^1}_{R^2}$	$-N$	$-N$	$-N$	$-N$	$-N$	$-N$	$-N$	$-N$	$-N\,O$

Scheme 1. The synthetic route of 1-hydroxyl-3-aminoalkoxy xanthone derivatives. Reagents and conditions: (i) $ZnCl_2$, $POCl_3$, 60 °C, 2 h; (ii) $Br(CH_2)_nBr$, K_2CO_3 reflux 24 h; (iii) appropriate amine, EtOH, reflux 2 h; (iv) CH_3I, $CHCl_3$, r. t., 24 h.

2.2. Biological activity

2.2.1. MTT assay and structure–activity relationships

Except for the insoluble lead compound **1**, the antiproliferative activities of all of the other synthesized compounds were tested *in vitro* on four human tumor cell lines, including CNE (nasopharyngeal neoplasm), BEL-7402 (liver cancer), MGC-803 (gastric cancer) and A549 (lung adenocarcinoma). 5-flurouracil (5-Fu) was used as the reference compound. The results were shown as IC_{50} value in Table 1.

The results in Table 1 indicated that most of the tested compounds exhibit effective cytotoxic activities against the four tested cancer cell lines with IC_{50} values at micromole concentration level. In the case of bromoalkoxyl substituted xanthone derivatives (**2a**–**2e**), no obvious cytotoxic activities were observed. It suggested that the introduction of bromoalkoxyl group to xanthone ring core was not helpful to improve its anticancer activity. In contrast, aminoalkoxy xanthone derivatives **3a**–**3i** show excellent anticancer activities with IC_{50} values in the range of 1.24–88.42 μM (except for compound **3i**). Comparing the IC_{50} values of compounds **3a**–**3i** with those of compounds **2a**–**2e**, it was obviously that the introduction of terminal amino groups could greatly improve their anticancer activities, which confirmed our designing idea. But for the case of corresponding quaternary ammonium derivatives **4a**–**4i**, their anticancer activities became weaker relative to compounds **3a**–**3i**. It might be due to that good water solubility of compounds **4a**–**4i** led to poor cytomembrane penetration.

To optimize the structure favorable for anticancer activities, two important structural factors were explored, including the types of terminal amino groups and the length of methylene linkers. Firstly, for compounds **3a**–**3e**, the xanthone ring core linked with terminal tetrahydropyrrol ring via different length of linker, were synthesized to investigate the influence of the length of side chains on the anticancer activities. The results showed that the length of side chains had no obviously regular influence on their anticancer activities. Compound **3c**, bearing a linker of $-(CH_2)_4-$ between xanthone pharmacophore and terminal amino group, showed potent inhibitory activities on the four tested cancer cell lines. Based on the potent inhibitory activities of compound **3c** and our previous experience [18], the length of the linker between xanthone pharmacophore and terminal amino group was fixed as $-(CH_2)_4-$ in the next step. That is, compounds **3c** and **3f**–**3i** containing four carbon spacers were tested on cancer cell lines for investigating the influence of different amino substituents on the antiproliferative activity. The IC_{50} values were shown in Fig. 2, it was obviously that compound **3g** with diethylamine substituent exhibit the best inhibitory activity in most cases, with IC_{50} value in the range of 3.57–20.07 μM. Interestingly, no notable inhibitory activities were observed for the morpholinyl substituted compound **3i**, with IC_{50} higher than 100 μM for all the tested cancer cell line, similar to our previous reports of other xanthones [17,18]. From the IC_{50} values of this series, it strongly suggested that the different terminal amino groups at the side chains had obvious impact on their anticancer activities, showing an order of diethylaminyl > dimethylaminyl > pyrrolidinyl > piperidinyl > morpholinyl.

Although further studies are necessary, a structure–activity relationship could be roughly established based on the discussion mentioned above. (1) The introduction of a *N*-containing side chain such as aminoalkoxy group to xanthone pharmacophore can greatly increase its anticancer activity, but further quaternarization of the amino group might decline its anticancer capability. (2) The

Table 1
Cytotoxic activity of the compounds **2a**–**4i** against four tested cancer cells.

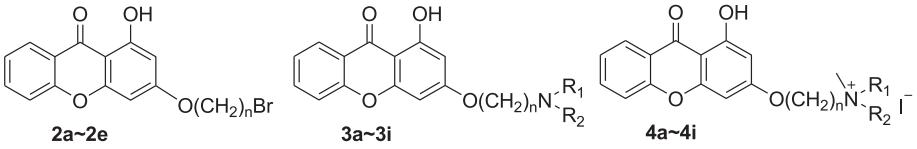

2a~2e **3a~3i** **4a~4i**

Compounds	IC_{50} (μM)			
	CNE	BEL-7402	MGC-803	A549
2a	>100	>100	21.5	>100
2b	>100	>100	28.9	>100
2c	85.61	67.9	22.7	>100
2d	>100	77.2	24.4	>100
2e	>100	>100	>100	>100
3a	11.32	14.61	5.63	12.85
3b	6.25	13.03	6.66	11.64
3c	5.97	20.83	4.50	18.51
3d	12.11	18.16	3.81	5.99
3e	1.24	17.94	5.32	8.94
3f	3.81	20.32	5.99	8.83
3g	3.63	20.07	3.57	7.57
3h	16.20	54.43	28.18	88.42
3i	>100	>100	>100	>100
4a	65.88	>100	83.34	>100
4b	>100	>100	9.66	>100
4c	>100	>100	8.04	19.49
4d	3.88	>100	12.73	10.71
4e	4.82	23.89	14.81	9.95
4f	38.48	>100	38.09	83.88
4g	>100	>100	4.61	12.99
4h	26.51	>100	5.13	19.21
4i	92.94	>100	17.61	>100
5-Fu	15.07	19.84	7.76	7.62

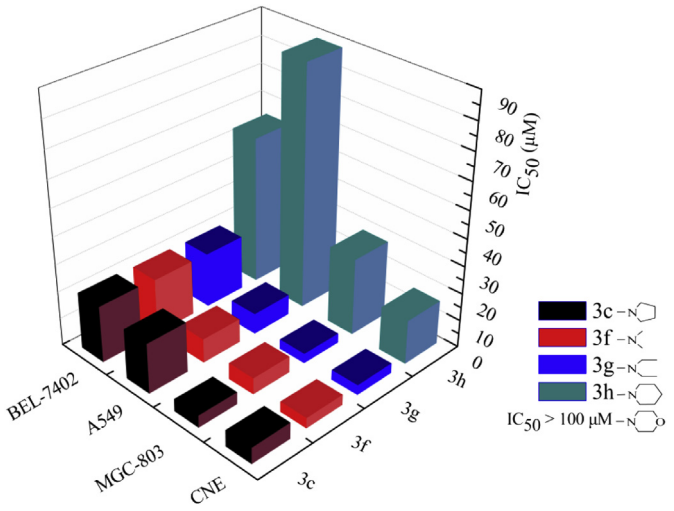

Fig. 2. Effects of terminal amino groups on cells proliferation.

length of the linker between xanthone pharmacophore and the terminal amino group has no obviously regular influence on its anticancer activity. (3) The anticancer activity of aminoalkoxy xanthone derivatives were greatly influenced by the structure of the terminal amino group.

Because compound **3g** was the most potent derivative possessing broad anticancer activities among all of the synthesized compounds, so its anticancer effect and preliminary anticancer mechanism on MGC-803 cell lines were further discussed in the following paragraphs.

2.2.2. *In vitro anticancer effect of compound **3g** on human gastric carcinoma MGC-803 cell*

The anticancer effect of compound **3g** on human gastric carcinoma MGC-803 cell was determined by MTT, morphological examination and clonogenic assay. MGC-803 cells were treated with compound **3g** at different concentrations for 24, 48, and 72 h, respectively, and then the cell viability was measured by MTT assay. Cell viability was calculated as a percentage of untreated cells (100%). Human MGC-803 cells treated with compound **3g** showed a time- and dose-dependent proliferation inhibition *in vitro* (Fig. 3A). At concentrations higher than1 μM, cell viability was statistically significantly decreased (all $P < 0.05$). The half maximal inhibitory concentration (IC_{50}) of compound **3g** on MGC-803 cells for 24, 48 and 72 h were 11.89, 3.57 and 1.82 μM, respectively. Moreover, inverted phase contrast microscopy was used to evaluate the cell survival and apoptotic changes of MGC-803 cells treated with compound **3g** for 72 h (Fig. 3B). The results showed that when MGC-803 cells were exposed to compound **3g** at 100 μM, the cells showed shrinkage and deformation while distribution of the cells was markedly sparseness as compared with the control group. To observe the delayed cytotoxic effects of this agent on MGC-803 cells, clonogenic survival assay was carried out. Colony formation was calculated as a percentage of untreated cells (100%). Experimental results revealed long-term proliferation inhibition effect of compound **3g** against MGC-803 cells by compound **3g** in a dose-dependent manner (Fig. 3C). Cell viability decreased significantly when the concentration of compound **3g** was above 1 μM (all $P < 0.001$). These results indicated that compound **3g** might be a potential anticancer agent.

2.2.3. *Compound **3g** induced apoptosis against MGC-803 cells*

Apoptosis is the process of programmed cell death that may occur in multicellular organisms. Biochemical events lead to characteristic cell changes (morphology) and death. These changes include blebbing, cell shrinkage, nuclear fragmentation, chromatin condensation, chromosomal DNA fragmentation and so on. Previous studies have showed that inducing apoptosis is one of the anticancer mechanisms of nature xanthone products [4]. In this study, apoptosis analysis of MGC-803 cells treated with compound **3g** were observed under a fluorescence microscope after being stained by Hochest 33258/Propidium iodide (PI). Hoechst 33258 limitedly passes the plasma membrane with intact membranes and

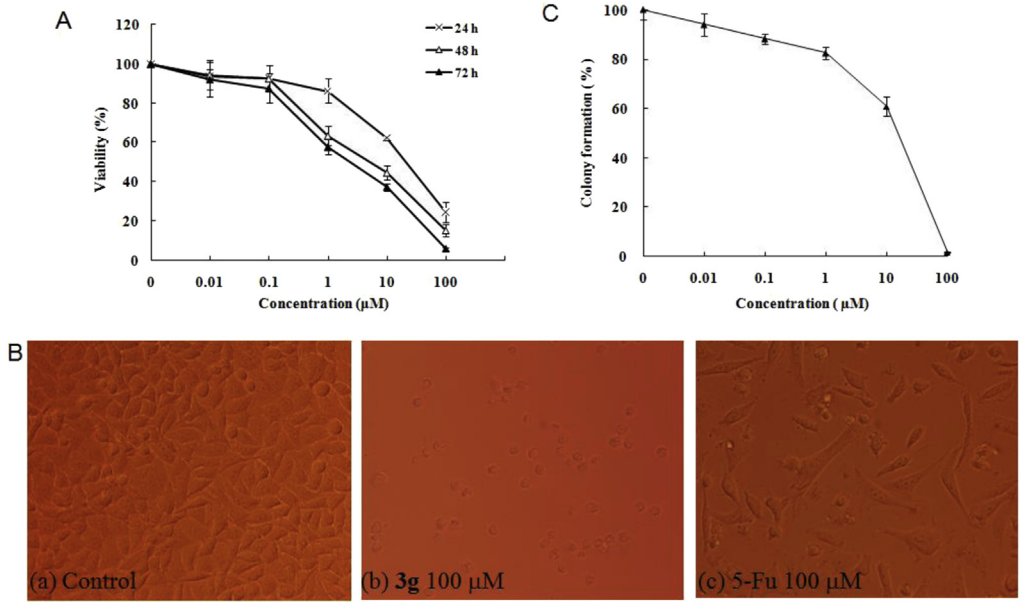

Fig. 3. Effects of compound **3g** on MGC-803 cell proliferation. A. Cell viability of MGC-803 cells treated with **3g** for 24 h, 48 h, and 72 h. Values were mean ± SD ($n = 5$); results are representative of three independent experiments. A two-tailed *t*-test was carried out. B. Images of MGC-803 cells with **3g** treated for 72 h (a) MGC-803 cells untreated as control, (b) MGC-803 cells treated with **3g** at 100 μM, (c) MGC-803 cells treated with 5-Fu at 100 μM. Original magnification ×100. C. **3g** inhibited the long-term proliferation of MGC-803 cells. Values were mean ± SD ($n = 3$); results are representative of three independent experiments.

readily enters cells with damaged membranes and stains DNA blue; whereas PI, a highly polar dye which is impermeable to cells with preserved membranes, stains DNA red. The nuclei of the living cells were shown light blue. Apoptotic cells were identified by nuclear condensation and/or fragmentation depending on the stage in the process (bright blue fluorescence indicates an early phase in apoptosis where the cell membrane is still intact, while a red fluorescence is an index for cells in the late phase of apoptosis, where the cell membrane integrity is lost). Necrotic cells were characterized by homogeneous red nucleus. After MGC-803 cells were exposed to compound **3g**, cell shrinkage was occurred in morphology as described above. With the incubation time prolonging to 24 h, nuclear condensation was observed. These characteristic cell changes indicated that compound **3g** induced apoptosis of MGC-803 cells. More than 1000 cells were counted, and apoptosis percentage was calculated according to it. Treatment with compound **3g** for 24 h induced MGC-803 cell apoptosis in a dose-dependent manner (Fig. 4). It appears that apoptosis associated cell death might be a main mechanism for compound **3g** to exhibiting proliferative inhibition to cancer cells.

2.2.4. Compound **3g** affected $[Ca^{2+}]_i$ of MGC-803 cells

Intracellular Ca^{2+} homeostasis is required for maintenance of cell survival. Apoptosis can be brought about by a loss of Ca^{2+} homeostatic control, but can also be finely tuned, positively or negatively, by more subtle changes in Ca^{2+} distribution within intracellular compartments. In its dual role, Ca^{2+} can either protect cells or cause their demise [20]. A biphasic mechanism of increased $[Ca^{2+}]_i$ has been reported in many studies, where moderate $[Ca^{2+}]_i$ elevations are antiapoptotic [21] but excessive $[Ca^{2+}]_i$ elevations are proapoptotic [22]. Diminutions in the concentrations of Ca^{2+} in cytosol, endoplasmic reticulum, or other intracellular compartments either directly or indirectly regulate apoptosis [23]. In this work, we measured $[Ca^{2+}]_i$ using the calcium indicator fura-2 AM,

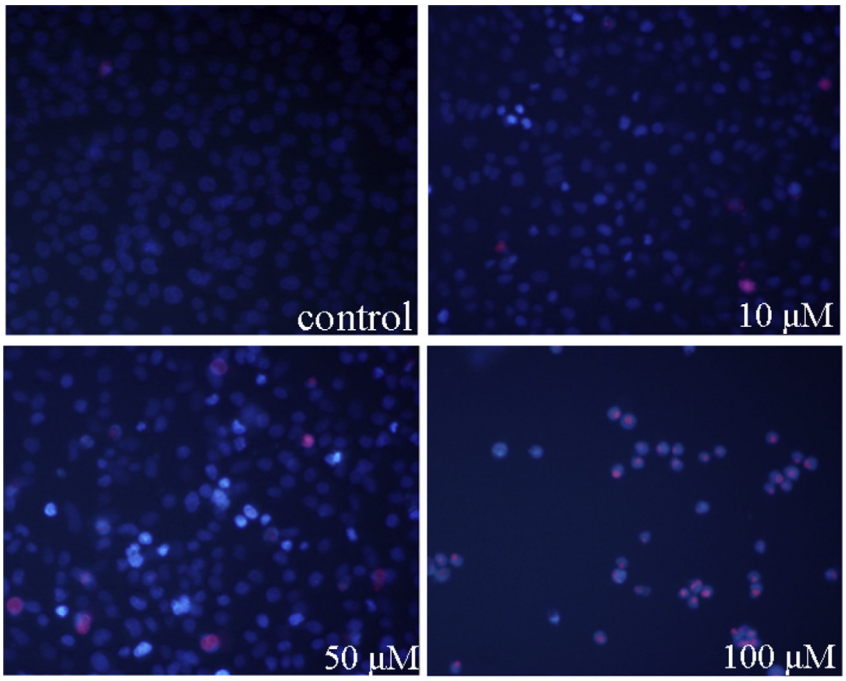

A

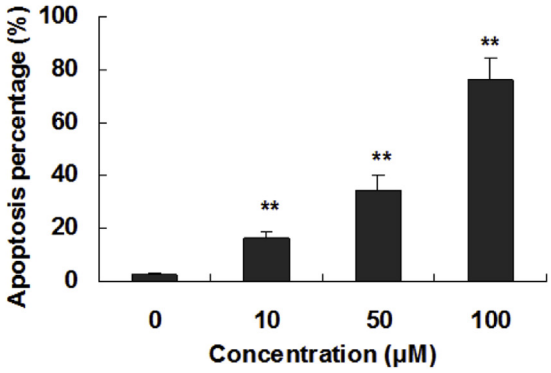

B

Fig. 4. Effect of compound **3g** on apoptosis in MGC-803 cells. (A) Morphological features of apoptosis and necrosis were examined after MGC-803 cells were exposed to **3g** for 24 h. (B) Apoptosis percentage. Data are means ± SD. $^*P < 0.05$; $^{**}P < 0.01$.

Ca^{2+}-sensitive fluorescent indicator, to examine whether $[Ca^{2+}]_i$ change were involved in the compound **3g** induced cancer cell apoptosis. F340,510/F380,510, which represents relative changes in intracellular $[Ca^{2+}]$, was visualized under a fluorospectrophotometer. After MGC-803 cells were treated with compound **3g** at 0, 10, 50 and 100 μM, respectively, altered $[Ca^{2+}]_i$ levels were examined. Distinct decrease of F340, 510/F380, 510 with compound **3g** treated at 10, 50 and 100 μM was showed in a dose-dependent manner when comparing with that in control (Fig. 5). The $[Ca^{2+}]_i$ changes induced by compound **3g** might be associated with one or more mechanisms including inhibiting calcium efflux from intracellular calcium pond, inducing calcium uptaking of endoplasmic reticulum (ER) or/and mitochondria, chelating intracellular calcium and other mechanisms. Further studies are needed to elucidate the potential mechanism.

2.2.5. Compound **3g** changed Δψm of MGC-803 cells

Mitochondrial dysfunction has been shown to participate in the induction of apoptosis and has even been suggested to be central to the apoptotic pathway. Opening of the mitochondrial permeability transition pore has been demonstrated to induce depolarization of the transmembrane potential (Δψm), release of apoptogenic factors and loss of oxidative phosphorylation. Loss of Δψm may be an early event or a consequence of the apoptotic-signaling pathway [24]. In this study, we measured mitochondrial membrane potential using the cationic fluorophore R123 to examine whether mitochondrial membrane potential change was involved in the compound **3g**-induced cancer cell apoptosis. For quantitation of R123 fluorescence as a semiquantitative assay of Δψ, fluorescent intensity of cells with compound **3g** addition was normalized to baseline values of control. Δψ decrease of MGC-803 cells treated with compound **3g** at 10, 50 and 100 μM was showed in a dose-dependent manner when compared with the control (Fig. 6).

3. Conclusion

In summary, a novel series of 1-hydroxyl-3-aminoalkoxy xanthone derivatives were designed, synthesized and evaluated for anticancer activities against four human cancer cell lines. The results showed that most of the compounds exhibited effective cytotoxic activities against the four tested cancer cell lines with the IC_{50} values at micromolar concentration level. The dimethylamine substituted compound **3g** demonstrated potent inhibitory activity with IC_{50} values of 3.63, 3.57, 7.57 and 20.07 against CNE, MGC-803, A549 and BEL-7402 respectively. The broad and significant anticancer activity shown by compound **3g** prompts our further investigation of the *in vitro* anticancer effect on human gastric carcinoma MGC-803 cell as well as its action mechanism. Compound **3g** exhibited dose- and time-dependent anticancer effects on MGC-803 cells through apoptosis, which might be associated with its decreasing intracellular calcium and the mitochondrial membrane potential. The 1-hydroxyl-3-aminoalkoxy xanthone derivatives have simple structure and are easy to be synthesized. These finding encouraged us to further optimize their structure and investigate their *in vivo* efficacy in animal model as well as the detail pharmacological mechanism.

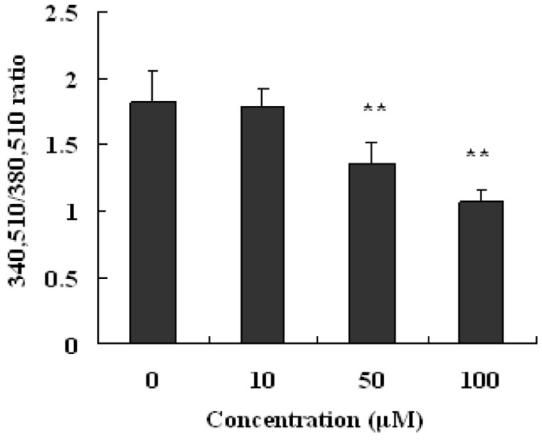

Fig. 5. Effect of compound **3g** on $[Ca^{2+}]_i$ level of MGC-803 cells.

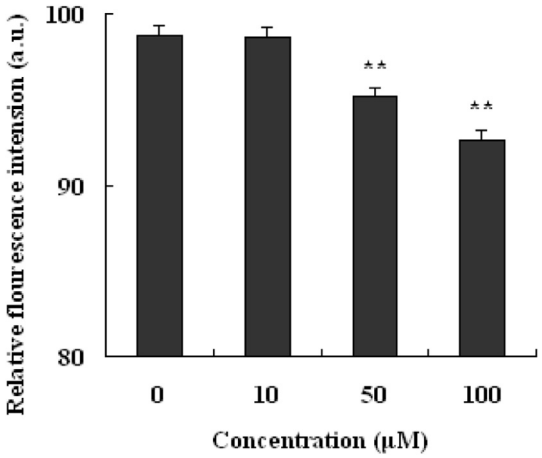

Fig. 6. Effect of compound **3g** on Δψ of MGC-803 cells.

4. Experiment section

4.1. General

All the solvents and reactants were of analytical grade and were used without further purification unless noted. All reactions were detected by thin layer chromatography (TLC) and spots were visualized by UV lamp or in iodine chamber. Melting points were measured in X-4 micro-melting point instrument and were uncorrected. IR spectra were taken on Nicolet ESP 360 FI-IR using KBr pellets. Direct MS spectra were performed on ESQUIRE HTC instrument. ^1H NMR and ^{13}C NMR spectra were recorded in $CDCl_3$ or DMSO-d_6 on Bruker AVANCE AV 500/125 MHz instruments. Chemical shifts were reported as δ ppm using tetramethylsilane (TMS) as the internal standard and couplings expressed in Hertz. Spin multiplicities were given as follows: s (singlet), d (doublet), t (triplet), m (multiplet), or br (broad). Column chromatography was accomplished on Qingdao silica gel (100–200 or 200–300 mesh).

4.2. Procedures for the synthesis of 1, 3-dihydroxyxanthone (**1**)

1, 3-dihydroxyxanthone (**1**) was prepared according to the literature [17,19]. Yield: 52%; m.p. 260–262 °C; IR (KBr), ν: 3327, 1654, 1610, 1570, 1491, 1470, 1445, 1222, 1163, 1078, 827, 762 cm^{-1}; ^1H NMR (500 MHz, δ, ppm, DMSO-d_6): 12.80 (s, 1H, OH-1), 11.07 (s, 1H, 3-OH), 8.10 (dd, J = 1.5, 8.0 Hz, 1H, H-8), 7.80–7.83 (m, 1H, H-6), 7.55 (d, J = 8.0 Hz, 1H, H-5), 7.42–7.45 (m, 1H, H-7), 6.37 (d, J = 2.1 Hz, 1H, H-4), 6.20 (d, J = 2.1 Hz, 1H, H-2).

4.3. General procedure for the synthesis of ω-bromoalkoxy substituted xanthones (**2a**–**2e**)

To a mixture of 1, 3-dihydroxyxanthone (1.01 g, 4.4 mmol) and K_2CO_3 (1.2 g, 8.8 mmol) in anhydrous acetone (15 mL), 1, 2-

dibromoethane or 1, 3-dibromopropane or 1, 4-dibromobutane or 1, 5-dibromopentane or 1, 6-dibromohexane (each 6.2 mmol) was added by a syringe. The reaction mixture was stirred under reflux for about 24 h until the starting material disappeared by TLC. After the reaction was completed, the reaction mixture was filtered, washed with acetone (30 mL) and then the filtrate was concentrated to afford the crude product, which could be recrystallized in acetone to give compound **2a**–**2e** respectively.

*4.3.1. 3-(2-Bromoethoxy)-1-hydroxy-9H-xanthen-9-one (**2a**)*

Yield: 51% from compound **1** and 1, 2-dibromoethane; a yellow solid; m.p.: 184–186 °C; ^{1}H NMR (500 MHz, δ, ppm, $CDCl_3$): 12.87 (s, 1H, OH), 8.25 (dd, J = 1.7, 7.9 Hz, 1H, H-8), 7.72 (ddd, J = 1.7, 7.2, 8.6 Hz, 1H, H-6), 7.43 (d, J = 8.6 Hz, 1H, H-5), 7.40–7.36 (m, 1H, H-7), 6.45 (d, J = 2.3 Hz, 1H, H-4), 6.35 (d, J = 2.3 Hz, 1H, H-2), 4.38 (t, J = 6.3 Hz, 2H, OC$\underline{H}_2$), 3.67 (t, J = 6.3 Hz, 2H, BrC$\underline{H}_2$); ^{13}C NMR (125 MHz, δ, ppm, $CDCl_3$): 180.9 (C-9), 165.0 (C-3), 163.7 (C-1), 157.8 (C-4a), 156.0 (C-4b), 135.1 (C-6), 125.9 (C-8), 124.1 (C-7), 120.7 (C-8a), 117.6 (C-5), 104.2 (C-8b), 97.4 (C-2), 93.4 (C-4), 68.1 (CH_2O), 28.2 (CH_2Br); IR (KBr) ν: 3438, 2940, 1656, 1608, 1570, 1464, 1287, 1161, 1081, 824 cm^{-1}; ESI-MS *m/z*: 335 [M+H]$^+$. Anal. Calcd for $C_{15}H_{11}BrO_4$: C, 53.76; H, 3.31. Found: C, 53.59; H, 3.33.

*4.3.2. 3-(3-Bromopropoxy)-1-hydroxy-9H-xanthen-9-one (**2b**)*

Yield: 58% from compound **1** and 1, 3-dibromopropane; a pale yellow solid; m.p.: 119–121 °C; ^{1}H NMR (500 MHz, δ, ppm, $CDCl_3$): 12.85 (s, 1H, OH), 8.24 (dd, J = 1.7, 7.9 Hz, 1H, H-8), 7.71 (ddd, J = 1.7, 7.3, 8.6 Hz, 1H, H-6), 7.42 (d, J = 8.6 Hz, 1H, H-5), 7.37 (dd, J = 7.3, 7.9 Hz, 1H, H-7), 6.43 (d, J = 2.2 Hz, 1H, H-4), 6.34 (d, J = 2.2 Hz, 1H, H-2), 4.20 (t, J = 5.9 Hz, 2H, OC$\underline{H}_2$), 3.61 (t, J = 6.4 Hz, 2H, BrC$\underline{H}_2$), 2.32–2.41 (m, 2H, OCH$_2$C$\underline{H}_2$CH$_2$ Br); ^{13}C NMR (125 MHz, δ, ppm, $CDCl_3$): 180.8 (C-9), 165.7 (C-3), 163.6 C-1), 157.7 (C-4a), 156.0 (C-4b), 135.0 (C-6), 125.8 (C-8), 124.0 (C-7), 120.6 (C-8a), 117.5 (C-5), 104.1 (C-8b), 97.5 (C-2), 93.2 (C-4), 66.0 (CH_2O), 31.9 (CH_2Br), 29.6 (CH_2); IR (KBr) ν: 3445, 2966, 1661, 1610, 1573, 1466, 1299, 1158, 1038, 825 cm^{-1}; APCI-MS *m/z*: 269 [M+H]$^+$. Anal. Calcd for $C_{16}H_{13}BrO_4$: C, 55.04; H, 3.75. Found: C, 55.07; H, 3.71.

*4.3.3. 3-(4-Bromobutoxy)-1-hydroxy-9H-xanthen-9-one (**2c**)*

Yield: 47% from compound **1** and 1, 4-dibromobutane; a yellow solid; m.p.: 133–135 °C; ^{1}H NMR (500 MHz, δ, ppm, $(CD_3)_2CO$-d_6): 12.88 (s, 1H, OH), 8.23 (dd, J = 1.5, 7.9 Hz, 1H, H-8), 7.87 (ddd, J = 1.5, 7.3, 8.5 Hz, 1H, H-6), 7.56 (d, J = 8.5 Hz, 1H, H-5), 7.49 (m, 1H, H-7), 6.59 (d, J = 2.0 Hz, 1H, H-4), 6.38 (d, J = 2.0 Hz, 1H, H-2), 4.25 (t, J = 6.2 Hz, 2H, OC$\underline{H}_2$), 3.63 (t, J = 6.6 Hz, 2H, C$\underline{H}_2$Br), 2.76–2.78 (m, 4H, C$\underline{H}_2$C$\underline{H}_2$); ^{13}C NMR (125 MHz, δ, ppm, $CDCl_3$): 180.8 (C-9), 166.0 (C-3), 163.5 (C-1), 157.7 (C-4a), 156.0 (C-4b), 135.0 (C-6), 125.8 (C-8), 124.0 (C-7), 120.6 (C-8a), 117.6 (C-5), 103.9 (C-8b), 97.4 (C-2), 93.2 (C-4), 67.6 (CH_2O), 33.2 (CH_2Br), 29.3 (CH_2), 27.6 (CH_2); IR (KBr) ν: 3546, 2959, 1663, 1609, 1572, 1469, 1299, 1158, 1081, 824 cm^{-1}; APCI-MS *m/z*: 363 [M+H]$^+$. Anal. Calcd for $C_{17}H_{15}BrO_4$: C, 56.22; H, 4.16. Found: C, 56.25; H, 4.13.

*4.3.4. 3-(5-Bromopentyloxy)-1-hydroxy-9H-xanthen-9-one (**2d**)*

Yield: 55% from compound **1** and 1, 5-dibromopentane; a yellow solid; m.p.: 129–131 °C; ^{1}H NMR (500 MHz, δ, ppm, $CDCl_3$): 12.85 (s, 1H, OH), 8.24 (dd, J = 1.7, 7.9 Hz, 1H, H-8), 7.70 (ddd, J = 1.7, 7.3, 8.5 Hz, 1H, H-6), 7.42 (d, J = 8.5 Hz, 1H, H-5), 7.34–7.40 (m, 1H, H-7), 6.41 (d, J = 2.2 Hz, 1H, H-4), 6.33 (d, J = 2.2 Hz, 1H, H-2), 4.06 (t, J = 6.4 Hz, 2H, OC$\underline{H}_2$), 3.45 (t, J = 6.7 Hz, 2H, C$\underline{H}_2$Br), 1.92–2.00 (m, 2H, OCH$_2$C$\underline{H}_2$CH$_2$ CH$_2$CH$_2$N), 1.83–1.89 (m, 2H, OCH$_2$CH$_2$CH$_2$C$\underline{H}_2$CH$_2$N), 1.62–1.68 (m, 2H, OCH$_2$ CH$_2$C$\underline{H}_2$CH$_2$CH$_2$N); ^{13}C NMR (125 MHz, δ, ppm, $CDCl_3$): 180.8 (C-9), 166.2 (C-3), 163.6 (C-1), 157.7 (C-4a), 156.1 (C-4b), 135.0 (C-6), 125.9 (C-8), 124.0 (C-7), 120.7 (C-8a), 117.6 (C-5), 103.9 (C-8b), 97.4 (C-2), 93.2 (C-4), 68.3 (OCH$_2$), 33.4 (CH_2Br), 32.4 (OCH$_2$C$\underline{H}_2$), 28.2(C$\underline{H}_2$CH$_2$Br), 24.7 (CH_2); IR (KBr) ν: 3461, 2943, 1662, 1608, 1572, 1481, 1299, 1166, 1038, 822 cm^{-1}; APCI-MS *m/z*: 377 [M+H]$^+$. Anal. Calcd for $C_{18}H_{17}BrO_4$: C, 57.31; H, 4.54. Found: C, 57.29; H, 4.56.

*4.3.5. 3-(6-Bromohexyloxy)-1-hydroxy-9H-xanthen-9-one (**2e**)*

Yield: 51% from compound **1** and 1, 6-dibromohexane; a yellow solid; m.p.: 139–140 °C; ^{1}H NMR (500 MHz, δ, ppm, $CDCl_3$): 12.85 (s, 1H, OH), 8.24 (dd, J = 1.7, 8.0 Hz,1H, H-8), 7.71 (ddd, J = 1.7, 7.2, 8.5 Hz, 1H, H-6), 7.42 (d, J = 8.5 Hz, 1H, H-5), 7.35–7.39 (m, 1H, H-7), 6.42 (d, J = 2.2 Hz, 1H, H-4), 6.33 (d, J = 2.2 Hz, 1H, H-2), 4.05 (t, J = 6.4 Hz, 2H, OC$\underline{H}_2$), 3.43 (t, J = 6.7 Hz, 2H, C$\underline{H}_2$Br), 1.88–1.94 (m, 2H, OCH$_2$C$\underline{H}_2$), 1.81–1.87 (m, 2H, C$\underline{H}_2$CH$_2$N), 1.50–1.56 (m, 4H, OCH$_2$CH$_2$C$\underline{H}_2$C$\underline{H}_2$CH$_2$ CH$_2$N); ^{13}C NMR (125 MHz, δ, ppm, $CDCl_3$): 180.8 (C-9), 166.3 (C-3), 163.6 (C-1), 157.8 (C-4a), 156.1 (C-4b), 134.9 (C-6), 125.9 (C-8), 124.0 (C-7), 120.7 (C-8a), 117.6 (C-5), 103.4 (C-8b), 97.4 (C-2), 93.3 (C-4), 68.5(OCH$_2$), 33.6 (CH_2Br), 32.7 (OC$\underline{H}_2$ CH$_2$), 28.9 (C$\underline{H}_2$CH$_2$Br), 27.9 (OCH$_2$CH$_2$ C$\underline{H}_2$), 25.2 (C$\underline{H}_2$CH$_2$CH$_2$Br); IR (KBr) ν: 3427, 2944, 1668, 1602, 1570, 1466, 1296, 1178, 1076, 823 cm^{-1}; APCI-MS *m/z*: 391 [M+H]$^+$. Anal. Calcd for $C_{19}H_{19}BrO_4$: C, 58.33; H, 4.89. Found: C, 58.27; H, 4.93.

*4.4. General procedure for the synthesis of 1-hydroxyl-3-aminoalkoxy xanthone derivatives (**3a**–**3i**)*

To a solution of **2a**–**2e** (0.7 mmol) in refluxed ethanol (15 mL), corresponding secondary amines (dimethylamine or diethylamine or pyrrolidine or piperidine or morpholine, 2.5 mmol) in ethanol (8 mL) was added dropwise by a syringe. The reaction mixture was stirred under reflux for about 0.5 h until the starting material disappeared monitored by TLC. On completion, the reaction mixture was cooled, concentrated under vacuum to afford the crude product, which could be recrystallized in acetone to give compound **3a**–**3e** respectively.

*4.4.1. 1-Hydroxy-3-(2-(pyrrolidin-1-yl)ethoxy)-9H-xanthen-9-one (**3a**)*

Yield: 88% from compound **2a** and pyrrolidine; a yellow solid; m.p.: 121–122 °C; ^{1}H NMR (500 MHz, δ, ppm, $CDCl_3$): 12.84 (s, 1H, OH), 8.24 (dd, J = 1.7, 8.0 Hz, 1H, H-8), 7.70 (ddd, J = 1.7, 7.3, 8.6 Hz, 1H, H-6), 7.42 (dd, J = 0.8, 8.6 Hz, 1H, H-5), 7.36 (ddd, J = 0.8, 7.3, 8.0 Hz, 1H, H-7), 6.45 (d, J = 2.3 Hz, 1H, H-4), 6.36 (d, J = 2.3 Hz, 1H, H-2), 4.21 (t, J = 5.9 Hz, 2H, OC$\underline{H}_2$), 2.95 (t, J = 5.8 Hz, 2H, OCH$_2$C$\underline{H}_2$N), 2.64–2.68 (m, 4H, α-CH_2 in pyrrole ring), 1.81–1.85 (m, 4H, β-CH_2 in pyrrole ring); ^{13}C NMR (125 MHz, δ, ppm, $CDCl_3$): 180.8 (C-9), 166.0 (C-3), 163.5 (C-1), 157.7 (C-4a), 156.0 (C-4b), 135.0 (C-6), 125.9 (C-8), 124.0 (C-7), 120.6 (C-8a), 117.6 (C-5), 104.0 (C-8b), 97.5 (C-2), 93.4 (C-4), 67.8 (OCH$_2$), 54.8 (2α-CH_2 in pyrrole ring), 54.7 (NCH$_2$), 23.5 (2β-CH_2 in pyrrole ring); IR (KBr) ν: 3418, 2957, 2780, 1656, 1609, 1570, 1467, 1364, 1296, 1161, 1076, 823, 759 cm^{-1}; APCI-MS *m/z*: 326 [M+H]$^+$. Anal. Calcd for $C_{19}H_{19}NO_4$: C, 70.14; H, 5.89; N, 4.31. Found: C, 70.11; H, 5.91; N, 4.33.

*4.4.2. 1-Hydroxy-3-(3-(pyrrolidin-1-yl)propoxy)-9H-xanthen-9-one (**3b**)*

Yield: 87% from compound **2b** and pyrrolidine; a yellow solid; m.p.: 107–109 °C; ^{1}H NMR (500 MHz, δ, ppm, $CDCl_3$): 12.81 (s, 1H, OH), 8.23 (dd, J = 1.7, 7.9 Hz, 1H, H-8), 7.69 (ddd, J = 1.7, 7.3, 8.5 Hz, 1H, H-6), 7.40 (d, J = 8.5 Hz, 1H, H-5), 7.35 (m, 1H, H-7), 6.42 (d, J = 2.2 Hz, 1H, H-4), 6.33 (d, J = 2.2 Hz, 1H, H-2), 4.12 (t, J = 6.4 Hz, 2H, OC$\underline{H}_2$), 2.63 (t, J = 7.4 Hz, 2H, OCH$_2$CH$_2$C$\underline{H}_2$N), 2.50–2.58 (m, 4H, α-CH_2 in pyrrole ring), 2.01–2.06 (m, 2H, OCH$_2$C$\underline{H}_2$CH$_2$N), 1.75–1.84 (m, 4H, β-CH_2 in pyrrole ring); ^{13}C NMR (125 MHz, δ, ppm, $CDCl_3$): 180.8 (C-9), 166.3 (C-3), 163.5 (C-1), 157.8 (C-4a), 156.1 (C-4b), 134.9 (C-6), 125.9 (C-8), 124.0 (C-7), 120.7 (C-8a), 117.6 (C-5), 103.9 (C-8b),

97.6 (C-2), 93.3 (C-4), 67.1 (OCH_2), 54.3 (2α-CH_2 in pyrrole ring), 52.8 (NCH_2), 28.6 (CH_2), 23.5 (2β-CH_2 in pyrrole ring); IR (KBr) ν: 3414, 2960, 2804, 1666, 1606, 1571, 1469, 1324, 1299, 1172, 1078, 823, 793 cm^{-1}; APCI-MS *m/z*: 340 $[M+H]^+$. Anal. Calcd for $C_{20}H_{21}NO_4$: C, 70.78; H, 6.24; N, 4.13. Found: C, 70.75; H, 6.27; N, 4.11.

4.4.3. 1-Hydroxy-3-(4-(pyrrolidin-1-yl)butoxy)-9H-xanthen-9-one (**3c**)

Yield: 85% from compound **2c** and pyrrolidine; a yellow solid; m.p.: 123–124 °C; ^1H NMR (500 MHz, δ, ppm, DMSO-d_6): 12.82 (s, 1H, OH), 8.22 (dd, *J* = 1.7, 7.9 Hz, 1H, H-8), 7.69 (ddd, *J* = 1.7, 7.2, 8.6 Hz, 1H, H-6), 7.40 (d, *J* = 8.6 Hz, 1H, H-5), 7.33–7.37 (m, 1H, H-7), 6.40 (d, *J* = 2.2 Hz, 1H, H-4), 6.31 (d, *J* = 2.2 Hz, 1H, H-2), 4.06 (t, *J* = 6.5 Hz, 2H, OCH_2), 2.48–2.54 (m, 6H, $N(CH_2)_3$), 1.83–1.89 (m, 2H, $OCH_2CH_2CH_2CH_2N$), 1.76–1.81 (m, 4H, β-CH_2 in pyrrole ring), 1.66–1.73 (m, 2H, OCH_2CH_2 CH_2CH_2 N); ^{13}C NMR (125 MHz, δ, ppm, $CDCl_3$): 180.7 (C-9), 166.3 (C-3), 163.5 (C-1), 157.7 (C-4a), 156.0 (C-4b), 134.9 (C-6), 125.9 (C-8), 123.9 (C-7), 120.7 (C-8a), 117.5 (C-5), 103.8 (C-8b), 97.5 (C-2), 93.2 (C-4), 68.5 (OCH_2), 56.0 (NCH_2), 54.2 (2α-CH_2 in pyrrole ring), 27.1 (OCH_2CH_2), 25.5 (NCH_2CH_2), 23.4 (2β-CH_2 in pyrrole ring); IR (KBr) ν: 3447, 2959, 2790, 1663, 1607, 1569, 1468, 1318, 1296, 1165, 1080, 823, 756 cm^{-1}. ESI-MS *m/z*: 354 $[M+H]^+$. Anal. Calcd for $C_{21}H_{23}NO_4$: C, 71.37; H, 6.56; N, 3.96. Found: C, 71.40; H, 6.55; N, 3.97.

4.4.4. 1-Hydroxy-3-(5-(pyrrolidin-1-yl)pentyloxy)-9H-xanthen-9-one (**3d**)

Yield: 92% from compound **2d** and pyrrolidine; a pale yellow solid; m.p.: 107–108 °C; ^1H NMR (500 MHz, δ, ppm, $CDCl_3$): 12.82 (s, 1H, OH), 8.22 (dd, *J* = 1.7, 7.9 Hz, 1H, H-8), 7.69 (ddd, *J* = 1.7, 7.2, 8.5 Hz, 1H, H-6), 7.40 (d, *J* = 8.5 Hz, 1H, H-5), 7.33–7.38 (m, 1H, H-7), 6.39 (d, *J* = 2.2 Hz, 1H, H-4), 6.31 (d, *J* = 2.2 Hz, 1H, H-2), 4.03 (t, *J* = 6.5 Hz, 2H, OCH_2), 2.44–2.52 (m, 6H, $N(CH_2)_3$), 1.81–1.87 (m, 2H, $OCH_2CH_2CH_2CH_2$ CH_2N), 1.74–1.80 (m, 4H, β-CH_2 in pyrrole ring), 1.56–1.63 (m, 2H, $OCH_2CH_2CH_2$ CH_2CH_2 N), 1.47–1.54 (m, 2H, $OCH_2CH_2CH_2CH_2CH_2$ N); ^{13}C NMR (125 MHz, δ, ppm, $CDCl_3$): 180.8 (C-9), 166.3 (C-3), 163.6 (C-1), 157.8 (C-4a), 156.1 (C-4b), 134.9 (C-6), 125.9 (C-8), 123.9 (C-7), 120.7 (C-8a), 117.6 (C-5), 103.9 (C-8b), 97.5 (C-2), 93.2 (C-4), 68.5 (OCH_2), 56.3 (NCH_2), 54.2 (2α-CH_2 in pyrrole ring), 28.9 (OCH_2CH_2), 28.4 (NCH_2CH_2), 24.0 ($NCH_2CH_2CH_2$), 23.4 (2β-CH_2 in pyrrole ring); IR (KBr) ν: 3430, 2949, 2793, 1662, 1608, 1571, 1468, 1316, 1299, 1166, 1082, 824, 763 cm^{-1}; APCI-MS *m/z*: 368 $[M+H]^+$. Anal. Calcd for $C_{22}H_{25}NO_4$: C, 71.91; H, 6.86; N, 3.81. Found: C, 71.85; H, 6.89; N, 3.83.

4.4.5. 1-Hydroxy-3-(6-(pyrrolidin-1-yl)hexyloxy)-9H-xanthen-9-one (**3e**)

Yield: 87% from compound **2e** and pyrrolidine; a pale yellow solid; m.p.: 104–105 °C; ^1H NMR (500 MHz, δ, ppm, $CDCl_3$): 12.86 (s, 1H, OH), 8.26 (dd, *J* = 1.6, 7.8 Hz, 1H, H-8), 7.71 (ddd, *J* = 1.6, 7.2, 8.4 Hz, 1H, H-6), 7.43 (d, *J* = 8.4 Hz, 1H, H-5), 7.39 (m, 1H, H-7), 6.42 (d, *J* = 2.0 Hz, 1H, H-4), 6.34 (d, *J* = 2.0 Hz, 1H, H-2), 4.06 (t, *J* = 6.0 Hz, 2H, OCH_2), 2.54–2.64 (m, 4H, α-CH_2 in pyrrole ring), 2.46–2.49 (m, 2H, $OCH_2CH_2CH_2CH_2CH_2CH_2N$), 1.79–1.88 (m, 6H, $OCH_2CH_2CH_2CH_2CH_2CH_2$ N), 1.61–1.62 (m, 2H, β-CH_2 in pyrrole ring), 1.50-1.53 (m, 2H, β-CH_2 in pyrrole ring), 1.41-1.43 (m, 2H, $OCH_2CH_2CH_2CH_2$ CH_2CH_2N); ^{13}C NMR (125 MHz, δ, ppm, $CDCl_3$): 180.7 (C-9), 166.3 (C-3), 163.5 (C-1), 157.7 (C-4a), 156.0 (C-4b), 134.9 (C-6), 125.8 (C-8), 123.9 (C-7), 120.6 (C-8a), 117.5 (C-5), 103.8 (C-8b), 97.4 (C-2), 93.2 (C-4), 68.6 (OCH_2), 56.5 (NCH_2), 54.2 (2α-CH_2 in pyrrole ring), 28.9 (OCH_2CH_2), 28.8 (NCH_2CH_2), 27.4 ($OCH_2CH_2CH_2$), 25.9 ($NCH_2CH_2CH_2$), 23.4 (2β-CH_2 in pyrrole ring); IR (KBr) ν: 3407, 2946, 2785, 1659, 1607, 1570, 1466, 1315, 1296, 1164, 1078, 823, 759 cm^{-1}; ESI-MS *m/z*: 382 $[M+H]^+$. Anal. Calcd for $C_{23}H_{27}NO_4$: C, 72.42; H, 7.13; N, 3.67. Found: C, 72.39; H, 7.15; N, 3.69.

4.4.6. 3-(4-(Dimethylamino)butoxy)-1-hydroxy-9H-xanthen-9-one (**3f**)

Yield: 85% from compound **2c** and dimethylamine; a yellow solid; m.p.: 121–122 °C; ^1H NMR (500 MHz, δ, ppm, $CDCl_3$): 12.96 (s, 1H, OH), 8.36 (d, *J* = 7.0 Hz, 1H, H-8), 7.81 (ddd, *J* = 1.7, 7.2, 8.4 Hz, 1H, H-6), 7.54 (d, *J* = 8.4 Hz, 1H, H-5), 7.48 (m, 1H, H-7), 6.53 (s, 1H, H-4), 6.44 (s, 1H, H-2), 4.18 (t, *J* = 5.8 Hz, 2H, OCH_2), 2.47 (t, *J* = 7.1 Hz, 2H, NCH_2), 2.33–2.37(m, 6H, $N(CH_2)_3$), 1.95–1.98 (m, 2H, $OCH_2CH_2CH_2$ CH_2N), 1.77–1.79 (m, 2H, $OCH_2CH_2CH_2CH_2N$); ^{13}C NMR (125 MHz, δ, ppm, $CDCl_3$): 180.7 (C-9), 166.2 (C-3), 163.5 (C-1), 157.7 (C-4a), 156.0 (C-4b), 134.8 (C-6), 125.8 (C-8), 123.8 (C-7), 120.6 (C-8a), 117.5 (C-5), 103.8 (C-8b), 97.4 (C-2), 93.2 (C-4), 68.4 (OCH_2), 59.2 (NCH_2), 45.4 ($2NCH_3$), 26.8 (OCH_2CH_2), 24.0 (NCH_2CH_2); IR (KBr) ν: 3649, 2935, 2757, 1661, 1608, 1569, 1467, 1316, 1296, 1163, 1079, 823, 758 cm^{-1}. APCI-MS *m/z*: 328 $[M+H]^+$. Anal. Calcd for $C_{19}H_{21}NO_4$: C, 69.71; H, 6.47; N, 4.28. Found: C, 69.69; H, 6.50; N, 4.27.

4.4.7. 3-(4-(Diethylamino)butoxy)-1-hydroxy-9H-xanthen-9-one (**3g**)

Yield: 86% from compound **2c** and diethylamine; a yellow solid; m.p.: 184–186 °C; ^1H NMR (500 MHz, δ, ppm, DMSO-d_6): 12.81 (s, 1H, OH), 8.17 (dd, *J* = 1.5, 8.0 Hz, 1H, H-8), 7.90 (ddd, *J* = 1.5, 7.2, 8.5 Hz, 1H, H-6), 7.63 (d, *J* = 8.5 Hz, 1H, H-5), 7.51 (m, 1H, H-7), 6.67 (d, *J* = 2.1 Hz, 1H, H-4), 6.43 (d, *J* = 2.1 Hz, 1H, H-2), 4.18 (t, *J* = 6.1 Hz, 2H, OCH_2), 2.91–3.02(m, 6H, $N(CH_2)_3$), 1.77–1.84 (m, 2H, $OCH_2CH_2CH_2CH_2N$), 1.70–1.75 (m, 2H, $OCH_2CH_2CH_2CH_2N$), 1.14 (t, *J* = 7.1 Hz, 6H, $N(CH_2CH_3)_2$); ^{13}C NMR (125 MHz, δ, ppm, $CDCl_3$): 180.7 (C-9), 166.3 (C-3), 163.5 (C-1), 157.7 (C-4a), 156.0 (C-4b), 134.9 (C-6), 125.9 (C-8), 123.9 (C-7), 120.7 (C-8a), 117.6 (C-5), 103.8 (C-8b), 97.5 (C-2), 93.2 (C-4), 68.6 (OCH_2), 52.5 (NCH_2), 46.9 ($N(CH_2CH_3)_2$), 27.1 (OCH_2CH_2), 23.6 (NCH_2CH_2), 11.7 ($N(CH_2CH_3)_2$); IR (KBr) ν: 3671, 2964, 2790, 1669, 1603, 1571, 1472, 1329, 1298, 1179, 1079, 821, 758 cm^{-1}. APCI-MS *m/z*: 356 $[M+H]^+$. Anal. Calcd for $C_{21}H_{25}NO_4$: C, 70.96; H, 7.09; N, 3.94. Found: C, 70.91; H, 7.11; N, 3.92.

4.4.8. 1-Hydroxy-3-(4-(piperidin-1-yl)butoxy)-9H-xanthen-9-one (**3h**)

Yield: 83% from compound **2c** and piperidine; a yellow solid; m.p.: 114–115 °C; ^1H NMR (500 MHz, δ, ppm, DMSO-d_6): 12.79 (s, 1H, OH), 8.15 (d, *J* = 7.8 Hz, 1H, H-8), 7.88 (ddd, *J* = 1.6, 7.3, 8.5 Hz, 1H, H-6), 7.61 (d, *J* = 8.5 Hz, 1H, H-5), 7.50 (dd, *J* = 7.3, 7.8 Hz, 1H, H-7), 6.65 (d, *J* = 1.7 Hz, 1H, H-4), 6.40 (d, *J* = 1.7 Hz, 1H, H-2), 4.14 (t, *J* = 6.6 Hz, 2H, OCH_2), 2.27–2.50 (m, 6H, $N(CH_2)_3$), 1.71–1.77 (m, 2H, OCH_2 $CH_2CH_2CH_2N$), 1.55–1.59 (m, 2H, $OCH_2CH_2CH_2CH_2N$), 1.47–1.52 (m, 4H, β-CH_2 in piperidine ring), 1.37–1.39 (m, 2H, γ-CH_2 in piperidine ring); ^{13}C NMR (125 MHz, δ, ppm, DMSO-d_6): 180.6 (C-9), 166.7 (C-3), 163.6 (C-1), 157.9 (C-4a), 156.1 (C-4b), 135.5 (C-6), 125.5 (C-8), 124.2 (C-7), 120.5 (C-8a), 117.6 (C-5), 103.4 (C-8b), 97.4 (C-2), 93.1 (C-4), 68.7 (OCH_2), 58.3 (NCH_2), 54.4 (2α-CH_2 in piperidine ring), 26.7 (OCH_2CH_2), 25.9 (2β-CH_2 in piperidine ring), 24.5 (NCH_2CH_2), 23.0 (γ-CH_2 in piperidine ring); IR (KBr) ν: 3447, 2959, 2790, 1662, 1607, 1569, 1468, 1319, 1296, 1165, 1080, 823, 756 cm^{-1}; APCI-MS *m/z*: 368 $[M+H]^+$. Anal. Calcd for $C_{22}H_{25}NO_4$: C, 71.91; H, 6.86; N, 3.81. Found: C, 71.94; H, 6.87; N, 3.80.

4.4.9. 1-Hydroxy-3-(4-morpholinobutoxy)-9H-xanthen-9-one (**3i**)

Yield: 84% from compound **2c** and morpholine; a yellow solid; m.p.: 143–144 °C; ^1H NMR (500 MHz, δ, ppm, $CDCl_3$): 12.86 (s, 1H, OH), 8.26 (dd, *J* = 1.6, 7.9 Hz, 1H, H-8), 7.73 (ddd, *J* = 1.6, 7.2, 8.5 Hz, 1H, H-6), 7.44 (dd, *J* = 0.4, 8.5 Hz, 1H, H-5), 7.40 (m, 1H, H-7), 6.43 (d, *J* = 2.2 Hz, 1H, H-4), 6.34 (d, *J* = 2.2 Hz, 1H, H-2), 4.10 (t, *J* = 6.4 Hz,

2H, OCH_2), 3.75 (t, J = 4.6 Hz, 4H, β-CH_2 in morphoing ring), 2.37–2.55 (m, 6H, NCH_2), 1.85–1.92 (m, 2H, $OCH_2CH_2CH_2CH_2N$), 1.69–1.75 (m, 2H, $OCH_2CH_2CH_2CH_2N$); ^{13}C NMR (125 MHz, δ, ppm, $CDCl_3$): 180.7 (C-9), 166.2 (C-3), 163.6 (C-1), 157.8 (C-4a), 156.1 (C-4b), 134.9 (C-6), 125.9 (C-8), 124.7 (C-7), 120.8 (C-8a), 117.5 (C-5), 103.9 (C-8b), 97.4 (C-2), 93.2 (C-4), 68.4 (OCH_2), 67.0 (2α-CH_2 in morphoing ring), 58.4 (NCH_2), 53.8 (2β-CH_2 in morphoing ring), 26.9 (OCH_2CH_2), 23.0 (NCH_2CH_2); IR (KBr) ν: 3441, 2944, 2773, 1664, 1605, 1569, 1467, 1317, 1297, 1167, 1077, 826, 765 cm^{-1}. ESI-MS m/z: 370 $[M+H]^+$. Anal. Calcd for $C_{21}H_{23}NO_5$: C, 68.28; H, 6.28; N, 3.79. Found: C, 68.26; H, 6.31; N, 3.81.

4.5. General procedure for the preparation of the corresponding quaternary ammonium derivatives (**4a**–**4i**)

To a solution of **3a**–**3i** (0.2 g) in chloroform (10 mL), iodomethane (1 mL) was added and then it was stirring at room temperature for about 3 days until the starting material disappeared by TLC. After the reaction was completed, the precipitate was filtrated, washed by chloroform (3 × 10 mL) and dried to give corresponding quaternary ammonium derivatives **4a**–**4i** respectively.

4.5.1. 1-(2-(1-Hydroxy-9-oxo-9H-xanthen-3-yloxy)ethyl)-1-methyl pyrrolidinium iodide (**4a**)

Yield: 93% from compound 3a and iodomethane; white solid; m.p.: 233–234 °C; ^{1}H NMR (500 MHz, δ, ppm, DMSO-d_6): 12.80 (s, 1H, OH), 8.16 (dd, J = 1.6, 7.9 Hz, 1H, H-8), 7.90 (ddd, J = 1.6, 7.3, 8.5 Hz, 1H, H-6), 7.63 (d, J = 8.5 Hz, 1H, H-5), 7.51 (m, 1H, H-7), 6.76 (d, J = 2.1 Hz, 1H, H-4), 6.51 (d, J = 2.1 Hz, 1H, H-2), 4.64 (t, J = 4.8 Hz, 2H, OCH_2), 3.88 (t, J = 4.8 Hz, 2H, OCH_2CH_2N), 3.55–3.65 (m, 4H, α-CH_2 in pyrrole ring), 3.12 (s, 3H, NCH_3), 2.10–2.16 (m, 4H, β-CH_2 in pyrrole ring); ^{13}C NMR (125 MHz, δ, ppm, DMSO-d_6): 181.4 (C-9), 165.4 (C-3), 163.4 (C-1), 158.2 (C-4a), 156.4 (C-4b), 137.3 (C-6), 126.2 (C-8), 125.8 (C-7), 120.6 (C-8a), 118.8 (C-5), 104.5 (C-8b), 98.7 (C-2), 94.6 (C-4), 65.8 (2α-CH_2 in pyrrole ring), 63.9 (OCH_2), 62.7(NCH_2), 49.3 (NCH_3), 22.0 (2β-CH_2 in pyrrole ring); IR (KBr) ν: 3467, 2959, 1656, 1606, 1573, 1470, 1323, 1294, 1169, 1081, 828, 787 cm^{-1}; ESI-MS m/z: 340 $[M+H]^+$. Anal. Calcd for $C_{20}H_{22}INO_4$: C, 51.40; H, 4.75; N, 3.00. Found: C, 51.37; H, 4.77; N, 3.02.

4.5.2. 1-(3-(1-Hydroxy-9-oxo-9H-xanthen-3-yloxy)propyl)-1-methylpyrrolidinium iodide (**4b**)

Yield: 94% from compound **3b** and iodomethane; white solid; m.p.: 231–232 °C; ^{1}H NMR (500 MHz, δ, ppm, DMSO-d_6): 12.77 (s, 1H, OH), 8.13 (dd, J = 1.6, 8.0 Hz, 1H, H-8), 7.88 (ddd, J = 1.6, 7.3, 8.6 Hz, 1H, H-6), 7.60 (dd, J = 0.8, 8.6 Hz, 1H, H-5), 7.49 (ddd, J = 0.8, 7.3, 8.0 Hz, 1H, H-7), 6.65 (d, J = 2.0 Hz, 1H, H-4), 6.40 (d, J = 2.0 Hz, 1H, H-2), 4.22 (t, J = 6.1 Hz, 2H, OCH_2), 3.48–3.59 (m, 6H, $N(CH_2)_3$), 3.06 (s, 3H, NCH_3), 2.20–2.30 (m, 2H, $OCH_2CH_2CH_2N$), 2.08–2.16 (m, 4H, β-CH_2 in pyrrole ring); ^{13}C NMR (125 MHz, δ, ppm, DMSO-d_6): 181.3 (C-9), 166.6 (C-3), 163.7 (C-1), 158.4 (C-4a), 156.6 (C-4b), 137.1 (C-6), 126.4 (C-8), 125.7 (C-7), 121.0 (C-8a), 118.9 (C-5), 104.4 (C-8b), 98.7 (C-2), 94.4 (C-4), 66.9 (OCH_2), 64.8 (2α-CH_2 in pyrrole ring), 61.4 (NCH_2), 48.8 (NCH_3), 24.3 (NCH_2CH_2), 22.2 (2β-CH_2 in pyrrole ring); IR (KBr) ν: 3432, 2960, 1657, 1604, 1571, 1467, 1324, 1295, 1172, 1076, 825, 782 cm^{-1}; ESI-MS m/z: 354 $[M+H]^+$. Anal. Calcd for $C_{21}H_{24}INO_4$: C, 52.40; H, 5.03; N, 2.91. Found: C, 52.37; H, 5.06; N, 2.94.

4.5.3. 1-(4-(1-Hydroxy-9-oxo-9H-xanthen-3-yloxy)butyl)-1-methylpyrrolidinium iodide (**4c**)

Yield: 89% from compound 3c and iodomethane; pale yellow solid; m.p.: 253–254 °C; ^{1}H NMR (500 MHz, δ, ppm, DMSO-d_6): 12.81 (s, 1H, OH), 8.18 (dd, J = 1.5, 7.9 Hz, 1H, H-8), 7.91 (ddd, J = 1.5, 7.3, 8.5 Hz, 1H, H-6), 7.63 (d, J = 8.5 Hz, 1H, H-5), 7.52 (dd, J = 7.3, 7.9 Hz, 1H, H-7), 6.70 (d, J = 2.1 Hz, 1H, H-4), 6.45 (d, J = 2.1 Hz, 1H, H-2), 4.20 (t, J = 6.1 Hz, 2H, OCH_2), 3.39–3.52 (m, 6H, $N(CH_2)_3$), 3.02 (s, 3H, NCH_3), 2.06–2.13 (m, 4H, β-CH_2 in pyrrole ring), 1.86–1.94 (m, 2H, $OCH_2CH_2CH_2CH_2N$), 1.78–1.85 (m, 2H, $OCH_2CH_2CH_2CH_2N$); ^{13}C NMR (125 MHz, δ, ppm, DMSO-d_6): 180.6 (C-9), 166.3 (C-3), 163.1 (C-1), 157.8 (C-4a), 156.0 (C-4b), 136.5 (C-6), 125.8 (C-8), 125.1 (C-7), 120.3 (C-8a), 118.2 (C-5), 103.6 (C-8b), 98.0 (C-2), 93.8 (C-4), 68.3 (OCH_2), 64.0 (2α-CH_2 in pyrrole ring), 63.2 (NCH_2), 48.1 (NCH_3), 25.9 (OCH_2CH_2), 21.6 (2β-CH_2 in pyrrole ring), 20.4 (NCH_2CH_2); IR (KBr) ν: 3425, 2954, 1665, 1607, 1569, 1483, 1325, 1294, 1165, 1081, 828, 780 cm^{-1}; ESI-MS m/z: 368 $[M+H]^+$. Anal. Calcd for $C_{22}H_{26}INO_4$: C, 53.34; H, 5.29; N, 2.83. Found: C, 53.30; H, 5.32; N, 2.85.

4.5.4. 1-(5-(1-Hydroxy-9-oxo-9H-xanthen-3-yloxy)pentyl)-1-methylpyrrolidinium iodide (**4d**)

Yield: 90% from compound **3d** and iodomethane; pale yellow solid; m.p.: 242–243 °C; ^{1}H NMR (500 MHz, δ, ppm, DMSO-d_6): 12.79 (s, 1H, OH), 8.16 (dd, J = 1.7, 7.9 Hz, 1H, H-8), 7.89 (ddd, J = 1.7, 7.2, 8.5 Hz, 1H, H-6), 7.61 (d, J = 8.5 Hz, 1H, H-5), 7.48–7.52 (m, 1H, H-7), 6.65 (d, J = 2.0 Hz, 1H, H-4), 6.41 (d, J = 2.0 Hz, 1H, H-2), 4.16 (t, J = 6.4 Hz, 2H, OCH_2), 3.41–3.51 (m, 6H, $N(CH_2)_3$), 3.00 (s, 3H, NCH_3), 2.05–2.12 (m, 4H, β-CH_2 in pyrrole ring), 1.76–1.84 (m, 4H, $OCH_2CH_2CH_2$ CH_2CH_2N), 1.42–1.49 (m, 2H, OCH_2CH_2 $CH_2CH_2CH_2N$); ^{13}C NMR (125 MHz, δ, ppm, DMSO-d_6): 180.6 (C-9), 166.5 (C-3), 163.1 (C-1), 157.8 (C-4a), 156.0 (C-4b), 136.5 (C-6), 125.8 (C-8), 125.1 (C-7), 120.3 (C-8a), 118.2 (C-5), 103.6 (C-8b), 98.0 (C-2), 93.8 (C-4), 68.8 (OCH_2), 64.0 (2α-CH_2 in pyrrole ring), 63.5 (NCH_2), 48.2 (NCH_3), 28.3 (OCH_2CH_2), 23.1 (NCH_2CH_2), 22.9 ($NCH_2CH_2CH_2$), 21.6 (2β-CH_2 in pyrrole ring); IR (KBr) ν: 3431, 2946, 1668, 1605, 1569, 1470, 1330, 1293, 1168, 1081, 829, 787 cm^{-1}; ESI-MS m/z: 382 $[M+H]^+$. Anal. Calcd for $C_{23}H_{28}INO_4$: C, 54.23; H, 5.54; N, 2.75. Found: C, 54.29; H, 5.51; N, 2.73.

4.5.5. 1-(6-(1-Hydroxy-9-oxo-9H-xanthen-3-yloxy)hexyl)-1-methylpyrrolidinium iodide (**4e**)

Yield: 89% from compound 3e and iodomethane; white solid; m.p.: 225–226 °C; ^{1}H NMR (500 MHz, δ, ppm, DMSO-d_6): 12.74 (s, 1H, OH), 8.11 (dd, J = 1.3, 7.9 Hz, 1H, H-8), 7.85 (ddd, J = 1.3, 7.2, 8.3 Hz, 1H, H-6), 7.57 (d, J = 8.3 Hz, 1H, H-5), 7.46 (dd, J = 7.2, 7.9 Hz, 1H, H-7), 6.59 (d, J = 2.1 Hz, 1H, H-4), 6.35 (d, J = 2.1 Hz, 1H, H-2), 4.10 (t, J = 6.4 Hz, 2H, OCH_2), 3.34–3.44 (m, 6H, $N(CH_2)_3$), 2.94 (s, 3H, NCH_3), 2.04 (s, 4H, β-CH_2 in pyrrole ring), 1.67–1.75 (m, 4H, $OCH_2CH_2CH_2CH_2CH_2$ CH_2N), 1.41–1.48 (m, 2H, $OCH_2CH_2CH_2CH_2CH_2CH_2N$), 1.29–1.36 (m, 2H, OCH_2 CH_2CH_2 $CH_2CH_2CH_2N$); ^{13}C NMR (125 MHz, δ, ppm, DMSO-d_6): 181.3 (C-9), 167.2 (C-3), 163.8 (C-1), 158.5 (C-4a), 156.7 (C-4b), 137.1 (C-6), 126.5 (C-8), 125.8 (C-7), 121.1 (C-8a), 118.9 (C-5), 104.3 (C-8b), 98.7 (C-2), 94.4 (C-4), 69.6 (OCH_2), 64.7 (2α-CH_2 in pyrrole ring), 64.3 (NCH_2), 48.9 (NCH_3), 29.3 (OCH_2CH_2), 26.7 (NCH_2CH_2), 26.1 ($OCH_2CH_2CH_2$), 24.0 (NCH_2 CH_2 CH_2), 22.3 (2β-CH_2 in pyrrole ring); IR (KBr) ν: 3464, 2943, 1662, 1603, 1568, 1469, 1328, 1294, 1168, 1078, 833, 783 cm^{-1}; ESI-MS m/z: 396 $[M+H]^+$. Anal. Calcd for $C_{24}H_{30}INO_4$: C, 55.07; H, 5.78; N, 2.68. Found: C, 55.04; H, 5.71; N, 2.65.

4.5.6. 4-(1-Hydroxy-9-oxo-9H-xanthen-3-yloxy)-N,N,N-trimethylbutan-1-aminiu-m iodide (**4f**)

Yield: 90% from compound 3f and iodomethane; white solid; m.p.: 232–233 °C; ^{1}H NMR (500 MHz, δ, ppm, DMSO-d_6): 12.77 (s, 1H, OH), 8.16 (dd, J = 1.6, 7.9 Hz, 1H, H-8), 7.90 (ddd, J = 1.6, 7.2, 8.6 Hz, 1H, H-6), 7.61 (d, J = 8.6 Hz, 1H, H-5), 7.52 (dd, J = 7.2, 7.9 Hz, 1H, H-7), 6.66 (d, J = 1.8 Hz, 1H, H-4), 6.42 (d, J = 1.8 Hz, 1H, H-2), 4.21 (t, J = 6.1 Hz, 2H, OCH_2), 3.38–3.44 (m, 2H, NCH_2), 3.09 (s, 9H, $N(CH_3)_3$), 1.85–1.92 (m, 2H, $OCH_2CH_2CH_2CH_2N$), 1.77–1.84 (m, 2H, $OCH_2CH_2CH_2$ CH_2N); ^{13}C NMR (125 MHz, δ, ppm, DMSO-d_6): 180.6

(C-9), 166.3 (C-3), 163.2 (C-1), 157.8 (C-4a), 156.0 (C-4b), 136.4 (C-6), 125.8 (C-8), 125.1 (C-7), 120.4 (C-8a), 118.2 (C-5), 103.7 (C-8b), 98.1 (C-2), 93.9 (C-4), 68.3 (OCH_2), 65.6 (NCH_2), 52.8 ($3NCH_3$), 25.8 ($OCH_2\underline{C}H_2$), 19.6 ($NCH_2\underline{C}H_2$); IR (KBr) ν: 3473, 2952, 1654, 1606, 1570, 1469, 1324, 1293, 1166, 1081, 830, 782 cm^{-1}; ESI-MS *m/z*: 342 $[M+H]^+$. Anal. Calcd for $C_{20}H_{24}INO_4$: C, 51.18; H, 5.15; N, 2.98. Found: C, 51.22; H, 5.17; N, 2.95.

4.5.7. N,N-diethyl-4-(1-hydroxy-9-oxo-9H-xanthen-3-yloxy)-N-methylbutan-1-a-minium iodide (**4g**)

Yield: 93% from compound **3g** and iodomethane; white solid; m.p.: 236–237 °C; ^{1}H NMR (500 MHz, δ, ppm, DMSO-d_6): 12.82 (s, 1H, O$\underline{H}$), 8.19 (dd, J = 1.5, 7.9 Hz, 1H, H-8), 7.91 (ddd, J = 1.5, 7.3, 8.4 Hz, 1H, H-6), 7.64 (d, J = 8.4 Hz, 1H, H-5), 7.52 (m, 1H, H-7), 6.71 (d, J = 2.0 Hz, 1H, H-4), 6.46 (d, J = 2.1 Hz, 1H, H-2), 4.21 (s, 2H, OCH_2), 3.28–3.33 (m, 6H, $N(CH_2)_3$), 2.93 (s, 3H, $NC\underline{H}_3$), 1.80–1.81 (m, 4H, $OCH_2\underline{C}H_2\underline{C}H_2CH_2N$), 1.23 (t, J = 6.8 Hz, 6H, $N(\underline{C}H_2C\underline{H}_3)_2$); ^{13}C NMR (125 MHz, δ, ppm, DMSO-d_6): 180.6 (C-9), 166.3 (C-3), 163.1 (C-1), 157.8 (C-4a), 156.1 (C-4b), 136.4 (C-6), 125.8 (C-8), 125.1 (C-7), 120.3 (C-8a), 118.2 (C-5), 103.7 (C-8b), 98.0 (C-2), 93.8 (C-4), 68.3 (OCH_2), 59.6 (NCH_2), 56.2 ($2NCH_2$), 47.1(NCH_3), 25.8 ($OCH_2\underline{C}H_2$), 18.8 ($NCH_2\underline{C}H_2$), 8.0 ($2CH_3$); IR (KBr) ν: 3436, 2954, 1663, 1607, 1571, 1469, 1320, 1296, 1166, 1082, 820, 781 cm^{-1}; ESI-MS *m/z*: 370 $[M+H]^+$. Anal. Calcd for $C_{22}H_{28}INO_4$: C, 53.13; H, 5.67; N, 2.82. Found: C, 53.17; H, 5.64; N, 2.80.

4.5.8. 1-(4-(1-Hydroxy-9-oxo-9H-xanthen-3-yloxy)butyl)-1-methylpiperidinium iodide (**4h**)

Yield: 89% from compound **3h** and iodomethane; pale yellow solid; m.p.: 235–236 °C; ^{1}H NMR (500 MHz, δ, ppm, DMSO-d_6): 12.75 (s, 1H, O$\underline{H}$), 8.12 (dd, J = 1.4, 7.8 Hz, 1H, H-8), 7.86 (ddd, J = 1.4, 7.4, 8.5 Hz, 1H, H-6), 7.58 (d, J = 8.5 Hz, 1H, H-5), 7.47 (dd, J = 7.4, 7.8 Hz, 1H, H-7), 6.63 (d, J = 1.8 Hz, 1H, H-4), 6.39 (d, J = 1.9 Hz, 1H, H-2), 4.14 (t, J = 6.0 Hz, 2H, OCH_2), 3.34–3.38 (m, 6H, $N(CH_2)_3$), 2.97 (s, 3H, $NC\underline{H}_3$), 1.75–1.81 (m, 8H, $OCH_2\underline{C}H_2\underline{C}H_2CH_2N$, β-$CH_2$ in piperidine ring), 1.47–1.52 (m, 2H, γ-CH_2 in piperidine ring); ^{13}C NMR (125 MHz, δ, ppm, DMSO-d_6): 180.6 (C-9), 166.3 (C-3), 163.1 (C-1), 157.8 (C-4a), 155.9 (C-4b), 136.5 (C-6), 125.8 (C-8), 125.1 (C-7), 120.3 (C-8a), 118.2 (C-5), 103.6 (C-8b), 98.0 (C-2), 93.8 (C-4), 68.3 (OCH_2), 62.3 (NCH_2), 60.5 (2α-CH_2 in piperidine ring), 47.6 (NCH_3), 25.8 ($OCH_2\underline{C}H_2$), 21.1 ($NCH_2\underline{C}H_2$), 19.7 (2β-CH_2 in piperidine ring), 18.4 (γ-CH_2 in piperidine ring); IR (KBr) ν: 3423, 2948, 1657, 1613, 1570, 1469, 1326, 1293, 1166, 1081, 828, 778 cm^{-1}; ESI-MS *m/z*: 382 $[M+H]^+$. Anal. Calcd for $C_{23}H_{28}INO_4$: C, 54.23; H, 5.54; N, 2.75. Found: C, 54.19; H, 5.57; N, 2.71.

4.5.9. 4-(4-(1-Hydroxy-9-oxo-9H-xanthen-3-yloxy)butyl)-4-methylmorpholin-4-ium iodide (**4i**)

Yield: 94% from compound **3i** and iodomethane; pale yellow solid; m.p.: 224–226 °C; ^{1}H NMR (500 MHz, δ, ppm, DMSO-d_6): 12.78 (s, 1H, O$\underline{H}$), 8.16 (dd, J = 1.7, 7.8 Hz, 1H, H-8), 7.90 (ddd, J = 1.7, 7.2, 8.6 Hz, 1H, H-6), 7.61 (d, J = 8.6 Hz, 1H, H-5), 7.52 (m, 1H, H-7), 6.67 (d, J = 2.0 Hz, 1H, H-4), 6.43 (d, J = 2.0 Hz, 1H, H-2), 4.21 (t, J = 5.8 Hz, 2H, OCH_2), 3.92–3.96 (m, 4H, β-CH_2 in morpholine ring), 3.55–3.56 (m, 2H, NCH_2), 3.44–3.45 (m, 4H, α-CH_2 in morpholine ring), 3.17 (s, 3H, $NC\underline{H}_3$), 1.86–1.90 (m, 2H, $OCH_2\underline{C}H_2CH_2CH_2N$), 1.79–1.84 (m, 2H, $OCH_2CH_2\,\underline{C}H_2CH_2$ N); ^{13}C NMR (125 MHz, δ, ppm, DMSO-d_6): 180.7 (C-9), 166.3 (C-3), 163.1 (C-1), 157.8 (C-4a), 156.0 (C-4b), 136.5 (C-6), 125.8 (C-8), 125.1 (C-7), 120.4 (C-8a), 118.2 (C-5), 103.7 (C-8b), 98.1 (C-2), 93.9 (C-4), 68.3 (OCH_2), 63.8 (NCH_2), 60.4 (2α-CH_2 in morpholine ring), 59.6 (2β-CH_2 in morpholine ring), 46.8 (NCH_3), 25.8 ($OCH_2\underline{C}H_2$), 18.3 ($NCH_2\underline{C}H_2$); IR (KBr) ν: 3439, 2959, 1665, 1607, 1570, 1469, 1326, 1293, 1167, 1081, 820, 786 cm^{-1}; ESI-MS *m/z*: 384 $[M+H]^+$. Anal. Calcd for $C_{22}H_{26}INO_4$: C, 51.67; H, 5.12; N, 2.74. Found: C, 51.61; H, 5.15; N, 2.71.

4.6. Cell culture

Cell lines were obtained from Shanghai Institutes for Biological Sciences, Chinese Academy of Sciences (Shanghai, China) and cultured as a monolayer in RPMI 1640 medium (Gibco BRL, Grand Island, NY, USA.) supplemented with 10% FBS (Gibco BRL, Grand Island, NY, USA.), penicillin (100 units/mL) and streptomycin (100 μg/mL), in a humid atmosphere at 37 °C with 95% air and 5% CO_2.

4.7. Cell viability assay

Inhibition of cell proliferation of xanthone derivatives (**2a**–**4i**) was measured by the MTT assay *in vitro* [25]. Briefly, cells were plated in 96-well culture plates at the density of 5000 cells per well in RPMI 1640 medium with 200 μL aliquots separately. After 24 h incubation, cells were treated with various concentrations of tested compounds for 48 h, 20 μL 5 mg/mL MTT was added to each well, and the cells were further incubated at 37 °C for another 4 h. The supernatant was discarded, and 150 μL DMSO was added into per well and then the absorbance (A) was measured at 490 nm. The cell viability ratio was calculated by the following equation: Inhibitory ratio (%) = $[(A_{control} - A_{treated})/(A_{control})] \times 100\%$. IC_{50} value was taken as the concentration that caused 50% inhibition of cell viabilities and calculated by the Logit method [26].

For anticancer effects of compound **3g** on MGC-803 cells, the compound was exposed to the cells for 24, 48 and 72 h respectively. Cell survival rates were calculated according to the following equation: Survival rate = (experimental absorbance value/control absorbance value) × 100%.

4.8. Colony formation assay

Delayed cytotoxic effects of agents on MGC-803 cells were determined using the clonogenic assay [27]. Briefly, after MGC-803 cells seeded in 6-well tissue culture plates (200 cells per well) were treated with compound **3g** for 24 h, all the cells were then incubated in humidified CO_2 atmosphere at 37 °C for 10 d. Colonies (more than >50 cells/colony) were counted and colony survival in percentage was calculated relative to the control (100%) group.

4.9. Fluorescence microscopy

MGC-803 cells were seeded in 24-well tissue culture plates and incubated for 24 h before treatment. Cells were exposed to compound **3g** for 24 h before stain with PI (20 μg/mL) and Hoechst 33258 (10 μg/mL, Sigma, St.Louis, MI) for 30 min. Images indicative of apoptosis were automatically captured with a fluorescence microscope (Leica DM4000B, Leica Microsystems, Nussloch, Germany). In each condition and experiment, minimally 1000 cells were counted for apoptosis percentage calculation.

4.10. Intracellular calcium ($[Ca^{2+}]_i$) measurement

Changes in $[Ca^{2+}]_i$ were measured by the ratiometric method in fura-2 AM-loaded cells [28]. Briefly, MGC-803 cells (1×10^6/mL) were dyed with 5 μM fura-2 AM (Sigma, St.Louis, MI) at 37 °C for 30 min in dark. The fluorescence intensity ratio of the Fluo-2 AM loaded cells was monitored using a dual-excitation fluorospectrophotometer (EL05113056, Cary Eclipse, Australia) at 340 and 380 nm for excitation and 510 nm for emission (F340, 510/F380, 510) after a pharmacological agent was administered and used as an index of $[Ca^{2+}]_i$. The results were normalized to baseline pretreatment values by dividing the average ratio and expressed as means ± SD.

4.11. Mitochondrial membrane potential ($\Delta\psi$) studies

The cationic fluorophore Rhodamine 123 (R123) concentrates in energized mitochondria and yields a punctate intracellular fluorescence in proportion to $\Delta\psi$ [30]. Briefly, MGC-803 cells were loaded with R123 (Sigma, St.Louis, MI) at 500 nM for 30 min at 37 °C, and then the cells were washed with experimental buffer and observed at 488 nm excitation and 535 nm emission. Compound **3g** was added once stable baseline fluorescence was attained. For quantitation of R123 fluorescence as a semiquantitative assay of $\Delta\psi$, fluorescent intensity of cells after compound **3g** addition was normalized to baseline values of control.

4.12. Statistical analyses

Data are presented as mean ± *SD* of duplicated analyses accompanied by the number of independent experiments. Statistical analyses were performed using two-tailed *t*-test. Differences at a *P* value of less than 0.05 were considered statistically significant.

Acknowledgments

This work was financially supported by grants from the National Natural Science Foundation of China (21002015), Natural Science Foundation of Guangxi (2010GXNSFB013013 and 2012GXNSFCB053001), Foundation of Guangxi Medicine Personnel Highlands (1107) and Key Laboratory for the Chemistry and Molecular Engineering of Medicinal Resources (Guangxi Normal University), Ministry of Education of the People's Republic of China (07109001-14 and, CMEMR2014-A01).

Appendix A. Supplementary data

Supplementary data associated with this article can be found in the online version, at http://dx.doi.org/10.1016/j.ejmech.2014.07.076. These data include MOL files and InChiKeys of the most important compounds described in this article.

References

[1] M.M.M. Pinto, M.E. Sousa, M.S.J. Nascimento, Xanthone derivatives: new insights in biological activities, Curr. Med. Chem. 12 (2005) 2517–2538.
[2] J.H. Cheng, A.M. Huang, T.C. Hour, S.C. Yang, Y.S. Pu, C.N. Lin, Antioxidant xanthone derivatives induce cell cycle arrest and apoptosis and enhance cell death induced by cisplatin in NTUB1 cells associated with ROS, Eur. J. Med. Chem. 46 (2011) 1222–1231.
[3] Y. Na, Recent cancer drug development with xanthone structures, J. Pharm. Pharmacol. 61 (2009) 707–712.
[4] X.M. Gao, T. Yu, M.Z. Cui, J.X. Pu, X. Du, Q.B. Han, Q.F. Hu, T.C. Liu, K.Q. Luo, H.X. Xu, Identification and evaluation of apoptotic compounds from Garcinia oligantha, Bioorg. Med. Chem. Lett. 22 (2012) 2350–2353.
[5] Y. Liu, Z.F. Ke, J.F. Cui, W.H. Chen, L. Ma, B. Wang, Synthesis, inhibitory activities, and QSAR study of xanthone derivatives as α-glucosidase inhibitors, Bioorg. Med. Chem. 16 (2008) 7185–7192.
[6] J.J. Omolo, M.M. Johnson, S.F. van Vuuren, C.B. de Koning, The synthesis of xanthones, xanthenediones, and spirobenzofurans: their antibacterial and antifungal activity, Bioorg. Med. Chem. Lett. 21 (2011) 7085–7088.
[7] D. Garcia-Rivera, R. Delgado, N. Bougarhe, G. Haegeman, W.V. Berghe, Gallic acid indanone and mangiferin xanthone are strong determinants of immunosuppressive anti-tumour effects of Mangifera indica L. bark in MDA-MB231 breast cancer cells, Cancer Lett. 305 (2011) 21–31.
[8] C.M.G. Azevedo, C.M.M. Afonso, J.X. Soares, S. Reis, D. Sousa, R.T. Lima, M.H. Vasconcelos, M. Pedro, J. Barbosa, L. Gales, M.M.M. Pinto, Pyranoxanthones: synthesis, growth inhibitory activity on human tumor cell lines and determination of their lipophilicity in two membrane models, Eur. J. Med. Chem. 69 (2013) 798–816.
[9] S. Woo, J. Jung, C. Lee, Y. Kwon, Y. Na, Synthesis of new xanthone analogues and their biological-Cytotoxicity, topoisomerase II inhibition, and DNA cross-linking study, Bioorg. Med. Chem. Lett. 17 (2007) 1163–1166.
[10] S. Woo, D.H. Kang, J.M. Nam, C.S. Lee, E.M. Ha, E.S. Lee, Y. Kwon, Y. Na, Synthesis and pharmacological evaluation of new methyloxiranylmethoxyxanthone analogues, Eur. J. Med. Chem. 45 (2010) 4221–4228.
[11] H.J. Cho, M.J. Jung, S. Woo, J. Kim, E.S. Lee, Y. Kwon, Y. Na, New benzoxanthone derivatives as topoisomerase inhibitors and DNA cross-linkers, Bioorg. Med. Chem. 18 (2010) 1010–1017.
[12] M. Hansen, S.J. Lee, J.M. Cassady, L.H. Hurley, Molecular details of the structure of a psorospermin-DNA covalent/intercalation complex and associated DNA sequence selectivity, JACS 118 (1996) 5553–5561.
[13] Y. Kwok, Q.P. Zeng, L.H. Hurley, Topoisomerase II-mediated site-directed alkylation of DNA by psorospermin and its use in mapping other topoisomerase II poison binding sites, Proc. Natl. Acad. Sci. U. S. A. 95 (1998) 13531–13536.
[14] S.-T. Woon, S. Zwain, M.A. Schooltink, A.L. Newth, B.C. Baguley, L.M. Ching, NF-kappa B activation in vivo in both host and tumour cells by the antivascular agent 5, 6-dimethylxanthenone-4-acetic acid (DMXAA), Eur. J. Cancer 39 (2003) 1176–1183.
[15] L.C.S. Wang, C.B. Reddy, B.C. Baguley, P. Kestell, R. Sutherland, L.M. Ching, Induction of tumor necrosis factor and interferon-γ in cultured murine splenocytes by the antivascular agent DMXAA and its metabolites, Biochem. Pharmacol. 67 (2004) 937–945.
[16] S. Gobbi, F. Belluti, A. Bisi, L. Piazzi, A. Rampa, A. Zampiron, M. Barbera, A. Caputo, M. Carrara, New derivatives of xanthenone-4-acetic acid: synthesis, pharmacological profile and effect on TNF-a and NO production by human immune cells, Bioorg. Med. Chem. 14 (2006) 4101–4109.
[17] W.L. Lan, J. C Wei, J.K. Qin, Z.M. Yang, G.F. Su, Z.K. Dai, Synthesis and biological evaluation of 1, 3-dihydroxyxanthone mannich base derivatives as potential antitumor agents, Lett. Drug Des. Discov. 10 (2013) 689–698.
[18] L. Luo, J.K. Qin, Z.K. Dai, S.H. Gao, Synthesis and biological evaluation of novel benzoxanthone derivatives as potential antitumor agents, J. Serb. Chem. Soc. 78 (2013) 1301–1308.
[19] P.K. Grover, G.D. Shah, R.C. Shah, Xanthones. IV. A new synthesis of hydroxyxanthones and hydroxybenzophenones, J. Chem. Soc. (1955) 3982–3985.
[20] S. Orrenius, B. Zhivotovsky, P. Nicotera, Regulation of cell death: the calcium-apoptosis link, Nat. Rev. Mol. Cell Biol. 4 (2003) 552–565.
[21] S. Yano, H. Tokumitsu, T.R. Soderling, Calcium promotes cell survival through CaM-K kinase activation of the protein-kinase-B pathway, Nature 396 (1998) 584–587.
[22] Z. Rekasi, T. Czompoly, A.V. Schally, F. Boldizsar, J.L. Varga, M. Zarandi, T. Berki, R.A. Horvath, P. Nemeth, Antagonist of growth hormone-releasing hormone induces apoptosis in LNCaP human prostate cancer cells through a Ca^{2+}-dependent pathway, Proc. Natl. Acad. Sci. U. S. A. 102 (2005) 3435–3440.
[23] G. Baffy, T. Miyashita, J.R. Williamson, J.C. Reed, Apoptosis induced by withdrawal of interleukin-3 (IL-3) from an IL-3-dependent hematopoietic cell line is associated with repartitioning of intracellular calcium and is blocked by enforced Bcl-2 oncoprotein production, J. Biol. Chem. 268 (1993) 6511–6519.
[24] J.D. Ly, D.R. Grubb, A. Lawen, The mitochondrial membrane potential (deltapsi(m)) in apoptosis, Apoptosis 8 (2003) 115–128.
[25] T. Mosmann, Rapid colorimetric assay for cellular growth and survival: application to proliferation and cytotoxicity assays, J. Immunol. Methods 65 (1983) 55–63.
[26] M. Wang, L. Zhang, X. Han, J. Yang, J. Qian, S. Hong, F. Samaniego, J. Romaguera, Q. Yi, Atiprimod inhibits the growth of mantle cell lymphoma *in vitro* and *in vivo* and induces apoptosis via activating the mitochondrial pathways, Blood 109 (2007) 5455–5462.
[27] L. Yeruva, C. Hall, J.A. Elegbede, S.W. Carper, Perillyl alcohol and methyl jasmonate sensitize cancer cells to cisplatin, Anticancer Drugs 21 (2010) 1–9.
[28] Z.K. Dai, J.K. Qin, J.E. Huang, Y. Luo, Q. Xu, H.L. Zhao, Tanshinone IIA activates calcium-dependent apoptosis signaling pathway in human hepatoma cells, J. Nat. Med. 66 (2012) 192–201.